

# Free Breathing Dynamic Contrast Enhanced 3D MRI with Resolved Respiratory Motion

Joseph Y. Cheng<sup>1,2</sup>, Tao Zhang<sup>1</sup>, John M. Pauly<sup>1</sup>, Shreyas S. Vasanawala<sup>2</sup>, and Michael Lustig<sup>3</sup>

<sup>1</sup>Electrical Engineering, Stanford University, Stanford, California, United States, <sup>2</sup>Radiology, Stanford University, Stanford, California, United States, <sup>3</sup>Electrical Engineering & Computer Sciences, University of California, Berkeley, California, United States

**PURPOSE:** Respiratory motion is a major issue in abdominal MRI, especially for pediatric patients who have difficulty performing breath-holds. The problem is exacerbated in lengthy scans, such as for dynamic contrast enhanced (DCE) MRI. Much of the previous work has been focused on reducing respiratory motion artifacts through reconstruction correction schemes. An alternative approach is resolving the motion. This approach has been previously proposed<sup>[1]</sup> where both cardiac and respiratory motion were resolved. Here, we adopt a similar approach to correct for respiratory motion in free breathing DCE-MRI by extending the data-acquisition space to an additional respiratory dimension and exploiting data redundancy to constrain the reconstruction.

**METHOD:** The discretized data consists of 5 dimensions: spatial (x,y,z), dynamic contrast  $n_{DCE}$ , and respiratory state  $n_{resp}$ . The scan acquisition is temporally constrained, especially for pediatrics, since most of the contrast dynamics occurs within 2 min after injection. Thus, the exam must be highly accelerated. Fortunately, redundancy improves with increasing dimensions<sup>[2]</sup>. Much like images are more redundant than audio and video more than images, our 5D-space is highly redundant.

**Algorithm:** For each TR, discrete values for  $n_{DCE}$  and  $n_{resp}$  are assigned to the corresponding readout. Time is segmented into  $N_{DCE}$  discrete bins for the  $n_{DCE}$ -dimension. Measured motion (with Butterfly<sup>[3]</sup>) is segmented into  $N_{resp}$  discrete bins for  $n_{resp}$  (Fig. 1). Images are reconstructed using CS-enhanced parallel imaging (PI). Given differing dynamics in  $n_{DCE}$  and in  $n_{resp}$ , different sparsity models are applied. The locally low-rank (LLR) constraint<sup>[4-6]</sup> is used in the  $n_{DCE}$ -dimension. The total variation (TV) penalty is used in the  $n_{resp}$ -dimension. The problem is a recovery of the 5D-image  $m$  from acquired k-space data  $y$ :

$$\arg \min_m \|Am - y\|_2 + \lambda_1 J_{resp}(m) + \lambda_2 J_{DCE}(m) \quad \text{where} \quad J_{resp}(m) = \|D_{n_{resp}} m\|_1 \\ J_{DCE}(m) = \sum_{n_{resp}} \sum_b \|C(b, n_{resp}) m\|_*$$

Matrix  $A$  consists of linear operations: applying the coil-sensitivity maps, taking the Fourier transform, and selecting the acquired samples. Function  $J_{resp}(m)$  is the TV penalty in  $n_{resp}$ -dimension where  $D_n$  is a finite-difference operator in dimension  $n$ . Function  $J_{DCE}(m)$  exploits LLR in  $n_{DCE}$ -dimension where  $b$  is a block in the spatial-dimension (we used a block size of 16x16),  $C(b, n_{resp})$  is the operator that reformats this block from a particular  $n_{resp}$  into a spatiotemporal matrix, and  $\|x\|_*$  is the nuclear norm of matrix  $x$ . Regularization parameters  $\lambda_1$  and  $\lambda_2$  are experimentally tuned.

**Setup:** Data were acquired using variable-density sampling and radial view-ordering (VDRad)<sup>[7]</sup>. Motion was measured using intrinsic navigation with the Butterfly<sup>[3]</sup> modification to a 3D Cartesian spoiled GRE sequence. Fat suppression was achieved using a spectrally selective fat-inversion pulse (TI = 9ms). Coil sensitivity maps were estimated using EPIRiT<sup>[8]</sup>. Our approach was compared to (1) soft-gated<sup>[9]</sup> LLR of a DCE<sup>[5]</sup> reconstruction and (2) L<sub>1</sub>-EPIRiT<sup>[8]</sup> of a lightly undersampled post-contrast scan.

**Experiment:** A 4-yr-old female was scanned on a 3T GE MR750 scanner using a 32-channel cardiac coil. Contrast was intravenously injected for the 2.7-min scan. The data were divided with  $N_{resp} = 8$  and  $N_{DCE} = 18$  (temporal resolution = 8.8 s). Specific scan parameters include TE/TR = 1.3/3.2 ms, flip angle = 15°, resolution = 1x1.4x2 mm<sup>3</sup>, FOV = 32x25.6x16 cm<sup>2</sup>, and bandwidth = ±100 kHz.

**RESULTS:** With respiratory-motion-resolved DCE-MRI, similar contrast dynamics were achieved compared to the DCE-only reconstruction. Our proposed approach yielded slightly sharper images due to the added TV penalty. Also, the acceptance window for respiratory motion in our method is much more strict through data binning. This strictness can be tolerated because of the additional  $n_{resp}$  to exploit sparsity conditions. Also, similar respiratory-motion dynamics were achieved compared to the post-contrast scans. The post-contrast scans resulted in slightly better image quality due to higher SNR from lower acceleration factors.

**DISCUSSION:** Computation is an issue for high-dimensional images. Fortunately, 3D Cartesian imaging enables slice-by-slice reconstruction along the fully encoded readout axis. This reduces the process to smaller and parallelizable 4D problems. Spatial sparsity, such as with spatial Wavelet transform<sup>[2]</sup>, can also be incorporated to further constrain the optimization at the cost of added computation. Lastly, the  $n_{resp}$ -dimension may provide more diagnostic information. Further investigation is required.

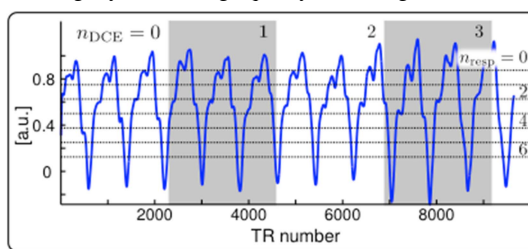


**FIG. 1: Data binning.** The acquired data is separated into  $n_{DCE}$  and  $n_{resp}$  bins. The entire scan is segmented by time into  $N_{DCE}$  different  $n_{DCE}$ -bins. The respiratory motion is used to divide the data into  $N_{resp}$  separate  $n_{resp}$ -bins. Here,  $N_{resp} = 8$ . Different bins can have very different acceleration factors.

**REFERENCES:** [1] L Feng et al, ISMRM 2013, p. 606. [2] M Lustig et al, MRM 2007; 58:1182-1195. [3] JY Cheng et al, MRM 2012; 68:1785-1797. [4] ZP Liang, ISBI 2007. [5] JD Trzasko and A Manduca, ISMRM 2011, p. 4371. [6] T Zhang et al, ISMRM 2013, p. 2624. [7] JY Cheng et al, ISMRM Data Workshop, 2013. proposed approach. [8] M Uecker, MRM 2013 (e-print). [9] KM Johnson et al, MRM 67: 1600-1608, 2012.

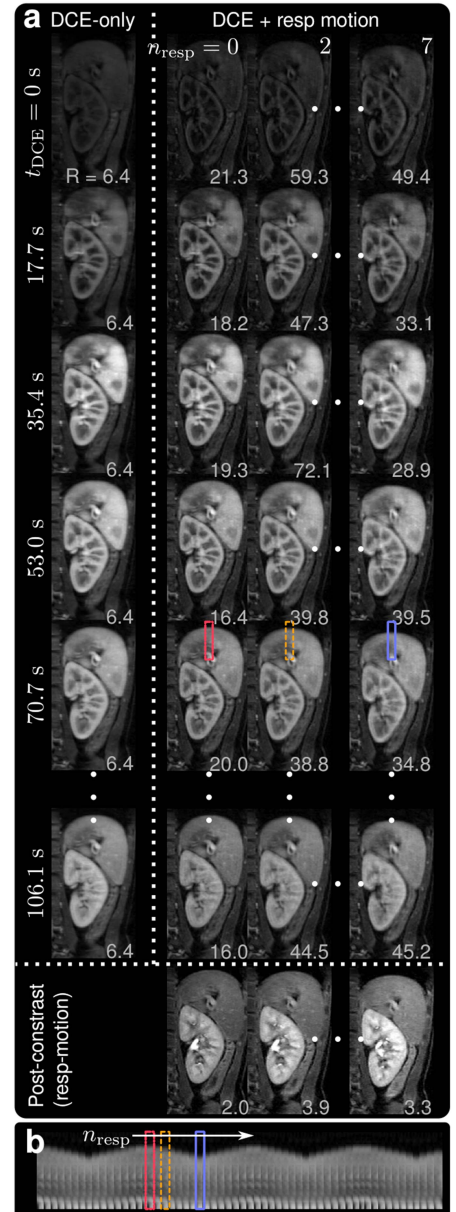


**FIG. 2: Free breathing DCE-MRI of a 4-yr-old female.** **a:** Comparison of DCE-MRI using soft-gated LLR (first column), motion-resolved DCE-MRI using proposed method (3  $n_{resp}$ -states shown in other columns), and post-contrast motion-resolved imaging using conventional PI/CS (last row). **b:** Cross-section from a single  $n_{DCE}$  illustrating the resolved respiratory motion (cross-sections are repeated to emphasize the periodic nature). Select time points are shown focusing on the enhancement of the kidney in the  $n_{DCE}$ -dimension ( $t_{DCE}$  corresponds to the actual time) and respiratory motion in the  $n_{resp}$ -dimension. The effective acceleration factor  $R$  is displayed on the bottom right corner of each image. Note the ability to depict comparable contrast dynamics and respiratory motion despite the high acceleration factor with our proposed approach.